Hydrogen Purification from Refinery Fuel Gas by Pressure Swing Adsorption

A. Malek and S. Farooq
Dept. of Chemical and Environmental Engineering, National University of Singapore, Singapore 119260

Hydrogen purification and recovery from various process streams constitutes the largest commercial use of pressure swing adsorption (PSA) technology. This study investigates the performance of a six-bed, dual-sorbent PSA operation for hydrogen purification from the refinery fuel gas. Major impurities are methane, ethane, propane and butane, and comprise 30–40% of the feed. The dual-sorbent PSA bed consists of an initial layer of silica gel adsorbent for trapping heavier hydrocarbons and a subsequent layer of activated carbon for removing lighter hydrocarbons. A numerical simulation model of the H_2-PSA process developed with all the essential features of the actual operation shows that butane is more strongly adsorbed on activated carbon than silica gel, and, hence, is less easily desorbed from the former using simple pressure reduction in the PSA cycle. Therefore, the initial layer serves to prevent butane from degrading the adsorptive capacity provided by activated carbon for other lighter hydrocarbons. The simulation model agrees well with the experimental results from a laboratory unit as well as with available H_2-PSA plant data from a refinery. The results also indicate the importance of heat effects in this process. Extensive parametric studies, which show effects of feed velocity and cycle time on the variation of product recovery and purity obtainable from the industrial unit, provide a valuable guide for its proper operation.

Introduction

In an earlier article (Malek and Farooq, 1997b), we discussed the development of a simulation model for a six-bed, ten-step pressure swing adsorption (PSA) process. The performance of the numerical model was verified with experimental results from a laboratory-scale PSA unit. Although the chosen configuration resembled that of an industrial operation for the purification of hydrogen from refinery fuel gas, a model system consisting of activated carbon adsorbent and a feed mixture containing three adsorbable hydrocarbon impurities, namely, methane, ethane, and propane in (inert) helium carrier, was considered as a precursor to modeling the actual industrial operation.

The use of helium in place of hydrogen was a measure of safety precaution in high pressure laboratory experiments. The simulation of an actual commercial operation must include hydrogen as carrier, which is weakly adsorbed on activated carbon. Moreover, refinery fuel gas normally contains trace amounts of higher molecular weight hydrocarbons, such as butane and aromatics, in addition to the light hydrocarbons considered in our previous study. These trace impurities can seriously degrade the capacity of the activated carbon adsorbent and, hence, the PSA performance, because they are more strongly adsorbed than the lighter hydrocarbons. Typically a silica gel layer is added to remove the heavier hydrocarbons prior to reaching the activated carbon layer, which is more suitable for the lighter hydrocarbons. These deficiencies in the model developed in our previous publication (Malek and Farooq, 1997b) have been addressed in this study.

The effect of the presence of butane in the feed stream on the overall PSA performance and the role of the silica gel layer have been examined in detail. The previous simulation model is first extended to include butane in the feed and an additional layer of silica gel adsorbent. The extended model is then verified with experimental results from the laboratory unit with helium as carrier. Finally, the model is further extended to simulate the actual industrial operation and its

Correspondence concerning this article should be addressed to S. Farooq.
Current address of A. Malek: Kvaerner R J Brown Pte Ltd., 73 Science Park Dr., Singapore 118254.

performance is compared with available plant data. It is shown that a mathematical model of an actual process, which is experimentally verified at various stages of development, can be efficiently used for the purpose of evaluating the effects of the design variables on the process performance.

Simulation of Dual-Sorbent PSA Process

The dual-sorbent PSA process was operated with the same cycle sequence adopted in the previous single-sorbent study (Malek and Farooq, 1997b). Therefore, the assumptions of the extended model are broadly similar to those made in the previous study. Only the modifications are elaborated here.

The main modification in the present dual-sorbent model is that the adsorbent physical properties, as well as the equilibrium parameters, mass-transfer, and heat-transfer kinetics for the adsorption of the hydrocarbons in the bed are now dependent on the location in the bed. In the dual-sorbent PSA studies conducted here, the beds contained an initial section of silica gel adsorbent, which amounted to 24.5% of the bed length, followed by activated carbon adsorbent that made up the rest of the bed (Figure 1). Hence, in the numerical solution of the PSA simulation model, the physical properties of the adsorbent, as well as the equilibrium and kinetic parameters, changed at a dimensionless length of 0.245 from the bed inlet. It is worth mentioning here that the equilibrium capacity of activated carbon for all the hydrocarbons is generally greater than that offered by silica gel (Malek, 1996). Thus, replacing a portion of the activated carbon adsorbent with silica gel resulted in a decrease in the overall adsorptive capacity provided by the columns for the hydrocarbons. Some relevant properties of the adsorbents used, the dimensions of the columns, and some other experimental details are given in Table 1.

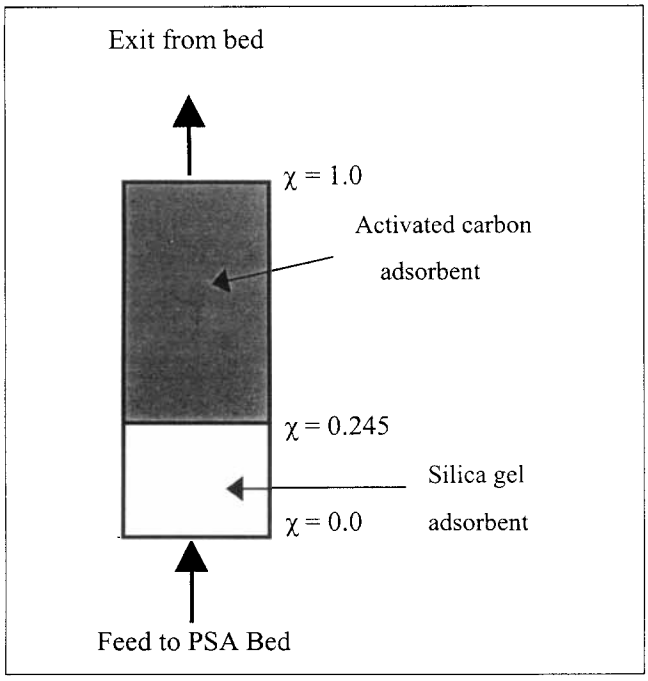

Figure 1. Dual-sorbent PSA bed.

Table 1. PSA Experimental Information

Column	*Jacketed stainless steel*
Internal diameter	4 cm
Length	40 cm
Adsorbent	*Activated carbon*
Apparent density*	0.87 $g \cdot cm^{-3}$
Particle porosity*	0.58
Mean pore radius*	18×10^{-8} cm (18 Å)
Specific surface area**	970 $m^2 \cdot g^{-1}$
Particle heat capacity**	0.95 J/g·K
Particle size	2.36–2.80 mm (Tyler equiv. 8-mesh and 7-mesh)
Bed void fraction	0.4
Adsorbent	*Silica gel*
Apparent density*	1.15 $g \cdot cm^{-3}$
Particle porosity*	0.44
Mean pore radius*	20×10^{-8} cm (20 Å)
Specific surface area*	666 $m^2 \cdot g^{-1}$
Particle heat capacity**	0.92 J/g·K
Particle size	2.36–2.80 mm (Tyler equiv. 8-mesh and 7-mesh)
Bed void fraction	0.4
Adsorbate	*Mixture of methane, ethane, propane and butane*
Carrier	*Helium*
Experimental range	
Interstitial gas velocity	0.427–0.715 cm/s
Cycle time	600–840 s
Pressure	P_H = 9.8 bar; P_L = 2.8 bar
Temperature	299.15 K

*Experimentally measured in this laboratory. Mean pore radius and specific surface area were determined using mercury porosimetry.
**Approximated from published literature.

The fourth hydrocarbon impurity in the feed, butane, is added to the extended Langmuir isotherm model in order to predict the multicomponent equilibrium. As with the other three components, the isotherm parameters for butane have also been taken from single-component measurements.

The linear driving force (LDF) approximation to model the particle uptake is also retained. As shown in Malek and Farooq (1997a) and Malek (1996), for the adsorption of C_1-C_4 in activated carbon adsorbent, $D_{e\,ave} = 0.0085$ cm^2/s, while for the same in silica gel adsorbent, $D_{e\,ave} = 0.0018$ cm^2/s.

The equilibrium isotherm parameters and mass- and wall heat-transfer parameters used in (Malek and Farooq, 1997b) and compiled in Table 2 of that publication are used in the present study without any change. The additional equilibrium and mass-transfer parameters required in the extended dual-sorbent model presented here are given in Table 2.

Other than the switch in process parameters at a dimensionless bed length of 0.245 from the inlet, the solution scheme for the dual-sorbent process is essentially similar to the procedure adopted for solving the single-sorbent process model described in the earlier study (Malek and Farooq, 1997b). It is pertinent to note that there are boundary constraints of continuous first- and second-order derivatives for mass and heat flow at the interface between the two adsorbent types (i.e., at $\chi = 0.245$) for the dual-sorbent PSA model. These constraints are intrinsically satisfied if that interface is between two collocation points. This was achieved with a choice of 19 collocation points. This choice was also found to provide a suitable compromise between minimizing the mag-

Table 2. Additional Equilibrium and Kinetic Parameters Necessary for the Extended Dual-Sorbent Model

Langmuir Isotherm Parameters†			
Silica Gel			
Methane	$q_s^* = 1.760$	$b_o = 5.050\times10^{-4}$	$(-\Delta H_A) = 12.804\times10^3$
Ethane	$q_s^* = 1.611$	$b_o = 2.340\times10^{-5}$	$(-\Delta H_A) = 25.6071\times10^3$
Propane	$q_s^* = 3.765$	$b_o = 1.840\times10^{-4}$	$(-\Delta H_A) = 20.120\times10^3$
Butane	$q_s^* = 2.344$	$b_o = 1.589\times10^{-5}$	$(-\Delta H_A) = 31.0112\times10^3$
Activated Carbon			
Butane	$q_s^* = 3.635$	$b_o = 5.568\times10^{-7}$	$(-\Delta H_A) = 44.412\times10^3$
Kinetic Parameter‡			
Silica gel: $D_{e,ave} = 0.0018$			

†Malek (1996).
‡Malek and Farooq (1997a).
Other equilibrium, mass-, and heat-transfer parameters used in the present simulation are same as those listed in Table 2 of Malek and Farooq (1997b).

nitude of oscillations in the numerical solution of the differential equations and the overall computation. The required CPU time for the solution of the nonisothermal, multicomponent, dual-sorbent PSA process on the Cray J916 Supercomputer (100 MHz) was expectedly much higher, being about 1,300 CPU s/cycle. On a SGI Power Challenge workstation running at 200 MHz, the same solution required about 850 CPU s/cycle. The increase in CPU time was mostly due to an increase in the number of impurities in the feed and not so much due to increase in the number of adsorbents. Cyclic steady state was attained in the simulation in about 130–150 cycles.

Experimental and Simulation Results

Figure 2 shows the experimental and simulation results of the six-bed PSA process with four adsorbable components in the feed (methane, ethane, propane, and butane). Figure 2a shows the results for a single-sorbent PSA process (activated carbon adsorbent), while Figure 2b shows the results for a dual-sorbent process (silica gel and activated carbon layers). The operating conditions for the two runs are otherwise the same and are given in Table 3. Experimental run number PAC6 is for a single-sorbent operation, while run number PAC7 is for a dual-sorbent operation. The main difference in the results of these two experimental runs is that the latter gives a somewhat earlier breakthrough. This is to be expected since less activated carbon adsorbent is available in the dual-sorbent process to retain the lighter hydrocarbon components in the feed. However, of particular importance is that throughout the experimental run the analysis of the vent stream (i.e., the blowdown and purge gas) composition for the single-sorbent process showed only a small presence of butane, whereas for the dual-sorbent process, butane was rejected more appreciably, together with the other hydrocarbons, during the blowdown and purge steps. Figure 3 shows a breakdown of the experimentally measured vent stream hydrocarbon composition for the two runs as a function of cycle number as determined by analyzing the collected samples using a Perkin Elmer Autosystem gas chromatograph fitted with a TCD and a Supelco Carboxen-1004 micropacked column.

Absence of butane in the vent stream for the single-sorbent run indicates that butane is strongly adsorbed by the activated carbon adsorbent, so much so that it is hardly desorbed under the regeneration conditions adopted here. Continuous operation under such a condition would naturally degrade the PSA performance, since butane would then accumulate in the beds (and penetrate deeper) and the total adsorption capacity provided by the beds for the other hydrocarbon compo-

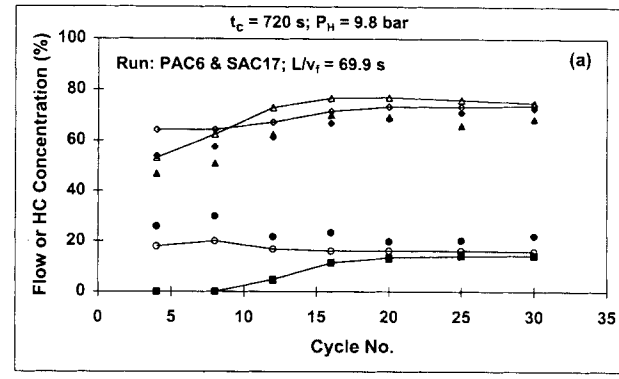

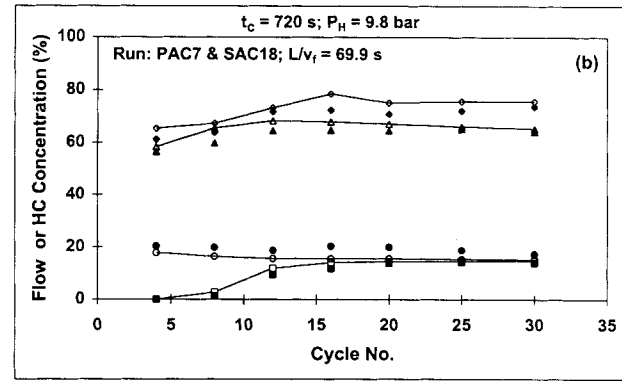

Figure 2. Comparison of experimental and simulation results for (a) single-sorbent and (b) dual-sorbent PSA performance with four adsorbable components.

■: product concentration; ♦: product recovery; ▲: vent concentration; ●: vent flow. Lines with open symbols are corresponding simulation results. Operating conditions are given in Table 3.

Table 3. Operating Conditions of Single- and Dual-Sorbent PSA Experimental and Simulation Runs*

Run No.	P_H (bar)	P_L (bar)	v_f (cm/s)	$X_{f1}/X_{f2}/X_{f3}/X_{f4}$	$t_{c1}/t_{c2}/t_{c3}$
Experimental					
PAC6	9.8	2.8	0.573	0.185/0.067/0.014/0.005	35/50/35
PAC7	9.8	2.8	0.573	0.185/0.067/0.014/0.005	35/50/35
Numerical Simulation					
SAC17	9.8	2.8	0.573	0.185/0.067/0.014/0.005	35/50/35
SAC18	9.8	2.8	0.573	0.185/0.067/0.014/0.005	35/50/35
SAC19	9.8	2.8	0.427	0.185/0.067/0.010/0.005	35/50/35
SAC20	9.8	2.8	0.715	0.185/0.067/0.010/0.005	35/50/35
SAC21	14.0	2.8	0.427	0.170/0.065/0.010/0.005	35/50/35
SAC22	18.0	2.8	0.427	0.170/0.065/0.010/0.005	35/50/35
SAC23	22.0	2.8	0.427	0.170/0.065/0.010/0.005	35/50/35

*PAC6 and SAC17 involved single-sorbent PSA operation while all the other runs involved a dual-sorbent process. All runs conducted with feed and column wall temperature of 299.15 K.

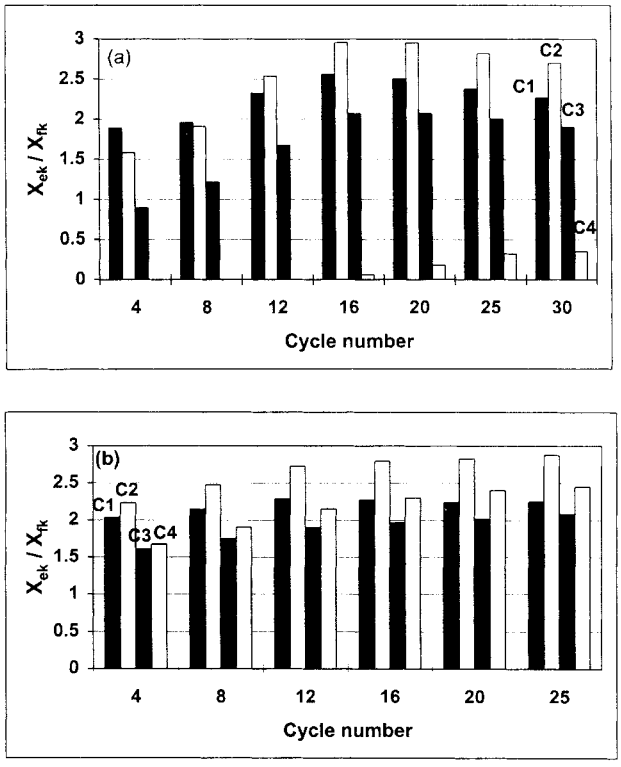

Figure 3. Breakdown of hydrocarbon composition in vent stream as a function of cycle number for (a) single-sorbent (Run PAC6) and (b) dual-sorbent (Run PAC7) PSA processes.

nents would diminish with time. In contrast, silica gel desorbs butane relatively readily. Ease or difficulty of desorption depends on the isotherm shape and butane isotherm is more favorable on activated carbon than on silica gel (Malek, 1996). Hence, the dual-sorbent system is more appropriate for operations where heavier molecular weight hydrocarbons are present.

The simulation results obtained (Figure 2) indicate that the mathematical model can closely predict the experimental PSA performance of the dual-sorbent system with four adsorbing components in the feed.

As a further study of the dual-sorbent PSA process, additional simulations were conducted (Table 3) to investigate the effects of various process parameters. Generally, the dual-sorbent system has an earlier breakthrough time as compared to the single-sorbent system (Malek and Farooq, 1997b). However, when the feed stream contains heavier hydrocarbons, the merit of the dual-sorbent system, as manifested in Figure 3, far exceeds the marginal loss in total bed capacity.

Figure 4 shows the simulated results of the effect of the high operating pressure, P_H, on product recovery and purity for the four-sorbate, dual-sorbent PSA system. These plots should be compared with the corresponding results for a feed gas containing three adsorbable components as shown in our previous publication (Figure 15 in Malek and Farooq, 1997b). Figure 4 shows that the product recovery drops from about 80% at 9.8 bar to just above 70% at about 16.0 bar, after which it levels off as the pressure is increased. There is a gradual increase in product purity with pressure. The results

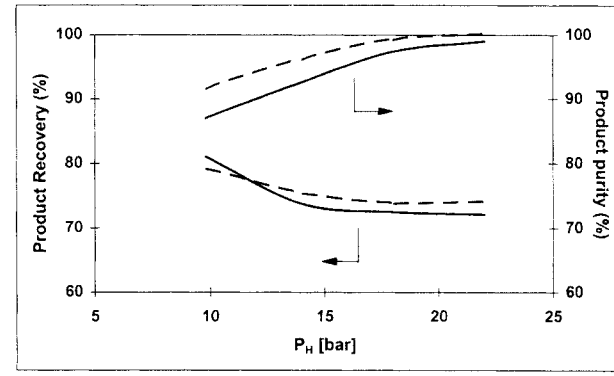

Figure 4. Product recovery and purity obtainable using the dual-sorbent, 6-bed PSA process as function of P_H.

Runs SAC19, SAC21, SAC22, and SAC23. Solid lines: nonisothermal operation; dashed lines: isothermal operation. Operating conditions are given in Table 3.

for the four-component, dual-sorbent PSA system generally show a slightly lower product purity for the same operating pressure as compared to the three-component, single-sorbent system. On the other hand, product recovery is about the same for the two operations. The purity results are expected since in the dual-sorbent operation, there is slightly earlier breakthrough of the lighter hydrocarbons due to a reduction in the total adsorptive capacity in the bed as a result of partial replacement of activated carbon with silica gel. It is also apparent that the amount of silica gel added in the column is just sufficient to prevent penetration of butane into the activated carbon section which could thereby cause rapid degradation of the separation characteristics.

It is interesting to consider, at this point, the effect of heat-transfer dynamics on the PSA performance. All the simulation results obtained earlier were for a nonisothermal column operation. In other words, there is a finite heat-transfer resistance at the column wall. As a result, the bed temperature profile varies with the cycle step. The simulation results for the product recovery and purity obtainable for the six-bed PSA process under isothermal conditions are also shown in Figure 4. In this case, there is no temperature variation in the bed, as it remains constant at all points and at every cycle step. The bed temperature is set equal to the feed temperature. The PSA simulation model can be easily configured to satisfy this condition by setting the temperature derivative equation to zero.

Under isothermal conditions, a higher product purity is generally obtainable as compared to nonisothermal operation. The difference in purity is largest at low operating pressure. The purity for the isothermal case gradually approaches that of the nonisothermal condition at higher operating pressure. This is expected since at the higher operating pressure there is very little breakthrough of hydrocarbons in both cases. The product recovery is slightly lower at low operating pressure ratio for the isothermal case, but quickly exceeds that obtained under nonisothermal operation as the operating pressure is increased. The difference in the plots for the isothermal and nonisothermal operations is a clear indication of the importance of heat effects in the PSA system being studied.

Performance of the Industrial PSA Unit

The six-bed PSA process in operation at a refinery in Singapore utilizes three different adsorbents, namely, activated alumina, silica gel, and activated carbon. The activated alumina layer, which amounts to less than 5% of bed volume, is used essentially to remove water vapor in the feed stream if any is present. In this study, it is assumed that dry feed enters the bed and that the activated alumina layer does not affect the bed capacity for the other hydrocarbon constituents in the feed stream to any appreciable extent. Thus only two layers of adsorbents are considered, namely, silica gel and activated carbon.

With respect to the cycle sequence, the operation of the industrial H_2-PSA unit follows the same steps and flow configuration used in the laboratory study. The simulation model for the industrial PSA process is the same as that for the dual-sorbent, four-component operation described earlier. Hydrocarbon constituents in the feed stream other than C_1-C_4 are ignored in this study since they are present in trace amounts, if at all. Apart from the bed dimensions, two other important differences that need to be considered in the industrial operation are the heat-transfer characteristic and the fact that hydrogen forms the bulk of the gas phase, instead of helium. Due to the small ratio of heat-transfer area to volume, the industrial PSA process operates more like an adiabatic process. As far as the simulation model is concerned, the required modification to account for this difference lies in the value of the wall heat-transfer coefficient, h_w. For adiabatic operation, h_w is set to zero in the simulation model.

The use of helium in place of hydrogen as the carrier gas in the laboratory experiments is the second important departure from the industrial operation. Limited experiments were conducted to study the impact of the presence of hydrogen on both the equilibrium and kinetics of hydrocarbon adsorption. Figure 5 shows the equilibrium adsorbed amount of hydrogen in activated carbon. The equilibrium amount was determined using both the dynamic column breakthrough and constant flow equilibrium desorption (DCBT and CFED) experiments (Malek and Farooq, 1996a). Although the adsorbed amount is small, there is some adsorption capacity for hydrogen in the sorbent. This is clear from the fact that the calculated adsorbed amount is higher than the amount present in the particle voids under the given pressure and temperature. The isotherm is, however, clearly linear over the range of interest. Figure 6 shows a comparison of two methane breakthrough curves obtained under the same operating conditions, but with helium as carrier in one and hydrogen as carrier in the other. In this case, the two curves are essentially similar, indicating a negligible effect of hydrogen on the equilibrium or kinetics of hydrocarbon adsorption on activated carbon. Based on these studies, the following assumptions are made for the simulation model of the industrial PSA process with hydrogen as the bulk gas:

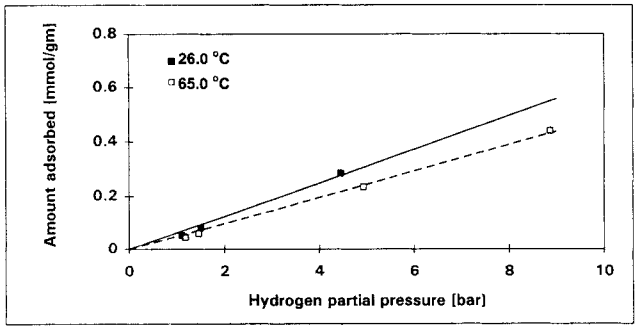

Figure 5. Adsorption equilibrium data of hydrogen on activated carbon at two different temperatures.

Lines: Henry's Law fit.

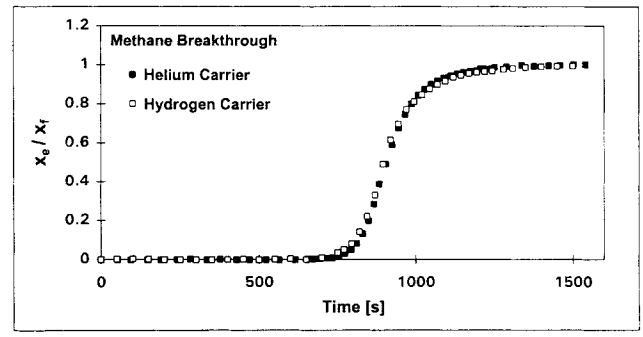

Figure 6. Comparison of methane breakthrough in activated carbon with helium and hydrogen as carriers.

a. Hydrogen has a very low adsorption capacity in activated carbon. The isotherm is linear and does not affect the capacity of the hydrocarbons, which are more strongly adsorbed.

b. Hydrogen is practically inert to silica gel.

c. Mass-transfer resistance for hydrogen is essentially negligible in both silica gel and activated carbon.

d. Hydrogen does not affect the adsorption kinetics of the hydrocarbons in both activated carbon and silica gel.

Hence, in the simulation model, the extended Langmuir model is used for computing multicomponent equilibria of hydrocarbon adsorption on both silica gel and activated carbon, with a linear isotherm model used for hydrogen adsorption on activated carbon. For silica gel, only the macropore volume capacity of hydrogen was taken into account, as was done for helium in all previous simulations. The Henry's Law parameters for the hydrogen-activated carbon adsorption equilibrium are given in Table 4. The Henry's Law equation is given as follows:

$$q_H^* = K_{oH} \exp\left(\frac{(-\Delta H_A)_H}{RT_f}\frac{1}{\theta}\right) P_B X_H \qquad (1)$$

As with the other components, the LDF model is adopted to characterize particle uptake. Since mass-transfer resistance for hydrogen adsorption is assumed to be negligible, an equilibrium model is used for hydrogen uptake as follows:

Table 4. Henry's Law Isotherm Parameters for Adsorption of Hydrogen on Activated Carbon

Isotherm Parameters	
$K_{oH} = 7.690 \times 10^{-3}$	$(-\Delta H_A)_H = 5.190 \times 10^3$

$$\frac{dY_H}{d\tau} = \frac{K_{oH}}{q_{s1}} \frac{\partial}{\partial \tau}\left(\exp\left(\frac{(-\Delta H_A)_H}{RT_f}\frac{1}{\theta}\right) P_B X_H\right)$$

$$= \frac{K_{oH}}{q_{s1}} \exp\left(\frac{(-\Delta H_A)_H}{RT_f}\right) \frac{\partial}{\partial \tau}\left(\exp\left(\frac{1}{\theta}\right) P_B\left(1 - \sum_i X_i\right)\right) \quad (2)$$

with $\gamma_H = 1$ for the hydrogen component. Thus, in the numerical solution, Eq. 2 above provides an additional term in solid loading calculation.

Similar to the simulation model for the laboratory unit, it is assumed that there is no interaction among the diffusing molecules of the adsorbable components. The pressure changing steps are modeled using linear driving force, with the proportionality coefficient chosen to fit measured plant bed pressure profiles. P_H and P_L are defined operating parameters. The same cycle sequence as described earlier is adopted for the industrial process. The substage durations for the simulations were taken to be equal to the durations used in the actual H_2-PSA operation.

Based on these assumptions, a series of numerical simulations of the H_2-PSA unit were conducted. The required CPU time for the simulation of the industrial, adiabatic, multicomponent, dual-sorbent H_2-PSA process on the Cray J916 Supercomputer was about 1,500 CPU s/cycle.

Figure 7 shows the results of the simulations in terms of product recovery and purity. The design specification for the industrial H_2-PSA unit as well as two sets of actual operating data obtained from the plant are also included in the figure for comparison. Table 5 provides the operating conditions for the plant data and simulation results. According to the design specification, the industrial unit should be operated at a P_H of 18.0 bar and a cycle time, t_c, of about 750 s. However, more often than not, the cycle time is reduced in actual PSA operations in order to contain the hydrocarbon fronts within the beds. The simulation model predictions, which are based on approximately the mean of these operating conditions, are in good agreement with the actual performance.

The recovery and purity plots shown in Figure 7 should be compared with the nonisothermal simulation results shown in Figure 4 for the laboratory-scale six-bed, dual-sorbent PSA unit. The general features of the plots for the industrial system are similar, showing an increasing trend in product purity and a drop in recovery with increasing pressure, with the recovery leveling off at just above 70% at pressures exceeding 15 bar. In the industrial system, however, the product purity is slightly lower than that for the nonisothermal, laboratory-scale operation. For the industrial H_2-PSA unit, it is also apparent that no advantage exists in operating the unit beyond a maximum pressure of about 18.0 bar, since the improvement in product purity beyond that pressure is marginal.

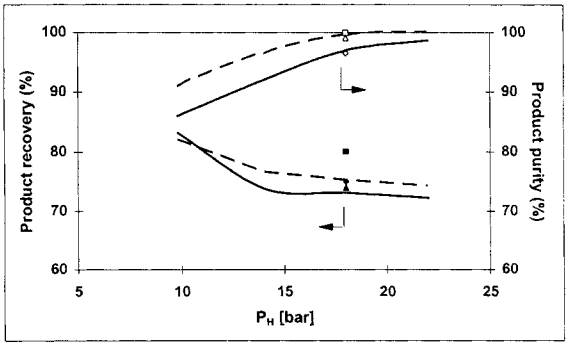

Figure 7. Comparison of product recovery and product purity from plant design specification, measured plant data and simulation model.

■: recovery from design specifications; ◆: recovery from plant data (11/23/92); ▲: recovery from plant data (11/22/92). Open symbols: product purity; solid lines: simulation results of adiabatic operation; dashed lines: simulation results of isothermal operation. Operating conditions are given in Table 5.

Table 5. Operating Conditions for Results Shown in Figure 7

Design Case	P_H (bar)	L/V_f (s)	T_f (K)	$X_{f1}/X_{f2}/X_{f3}/X_{f4}$	$t_{c1}/t_{c2}/t_{c3}$
SRC Plant Data					
	18.0	69.0	311.15	0.20/0.07/0.06/0.03	35/58/35
Nov. 22, 1992	18.0	71.4	306.15	0.15/0.04/0.02/0.01	32/52/32
Nov. 23, 1992	18.0	74.1	307.15	0.15/0.06/0.03/0.016	32/52/32
Simulation					
	9.8 – 22.0	69.8	308.15	0.17/0.065/0.02/0.01	35/50/35

Figure 7 also includes the isothermal model results for the industrial unit. As seen for the laboratory unit, the isothermal model also generally predicts higher product recovery and purity for the industrial unit. It is interesting to note that the recovery and purity data for the design case are closer to the isothermal simulation results, although the predicted recovery is somewhat lower. The distinction is less definite for the limited actual plant data, but it is perhaps not unreasonable to conclude that the isothermal model will most likely lead to an underdesign of the PSA unit.

In the actual industrial PSA process, the two other important operating variables are the feed velocity to the columns, v_f, and the cycle time (specifically the duration of the high-pressure adsorption step). It would, therefore, be beneficial to study the effects of these variables on the PSA performance as quantified by the product recovery and purity. Figure 8 shows the variations in the recovery and purity as functions of L/v_f and the PSA cycle time, t_c. The operating conditions for the simulation results in the figure are given in Table 6.

The simulation results show that the product recovery increases with feed velocity (decreasing L/v_f ratio), as expected. The recovery is also generally a monotonically increasing function of cycle time. On the other hand, the dependence of product purity on the feed velocity and cycle time is slightly more intricate. Increasing cycle time sharpens the concentration front and increases product purity when operating far from breakthrough. In this range, the bed is not fully utilized, which reduces the practical importance of the gain in purity. Increasing both feed velocity and cycle time reduces the product purity in the chosen operating range. The quantitative decrease in purity is dependent on the extent of breakthrough of the hydrocarbon components. For the lower velocity run, there is insignificant breakthrough of the hydrocarbons, and, thus, the purity drops only marginally, remaining above 95%. At higher velocities, the hydrocarbons begin to break through to a larger extent, as shown by the plots for $L/v_f = 93.7$ s and $L/v_f = 71.4$ s. For the former case, there is a rapid drop in the purity due to the sharp breakthrough of methane as the cycle time is increased. For the latter condi-

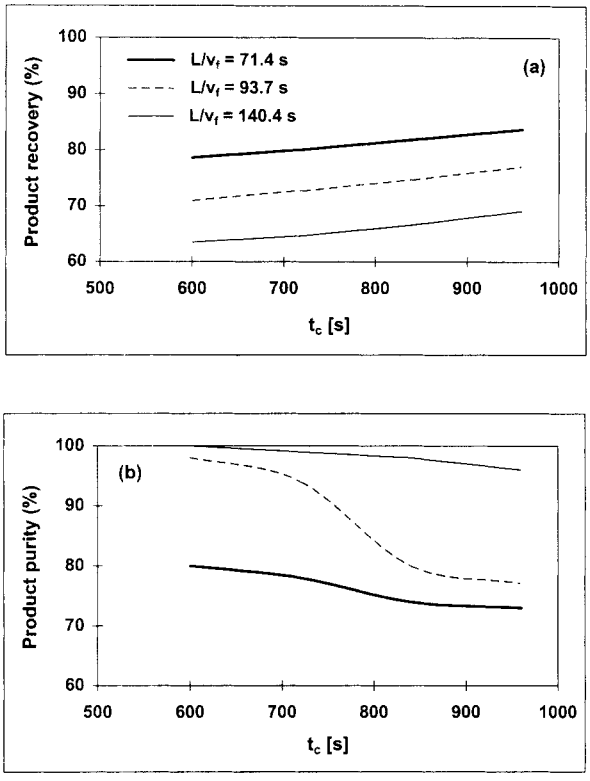

Figure 8. Effect of cycle time, t_c, on (a) product recovery and (b) product purity at different L/v_f ratios for dual-sorbent PSA process.

Operating conditions are given in Table 6.

tion, on the other hand, there is substantial breakthrough of hydrocarbons, with complete methane breakthrough, even at a short cycle time as a result of the high feed velocity. Hence, the purity for this case is consistently low. Figure 8 provides a useful guide for the proper operation of the industrial PSA process in terms of maintaining high product recovery as well as purity by varying the relevant operating conditions. In particular, it is possible to achieve very high ($\geq 99.9\%$) product purity by operating at low cycle time and feed velocity.

The movements of the concentration wave fronts in the adsorbed phase as a function of cycle number are shown in

Table 6. Operating Conditions for Dual-Sorbent PSA Simulation Runs in Figure 8*

Run No.	P_H (bar)	P_L (bar)	L/v_f (s)	$X_{f1}/X_{f2}/X_{f3}/X_{f4}$	$t_{c1}/t_{c2}/t_{c3}$
SAC24	18.0	2.8	140.4	0.17/0.065/0.03/0.01	35/30/35
SAC25	18.0	2.8	140.4	0.17/0.065/0.03/0.01	35/50/35
SAC26	18.0	2.8	140.4	0.17/0.065/0.03/0.01	35/70/35
SAC27	18.0	2.8	140.4	0.17/0.065/0.03/0.01	35/90/35
SAC28	18.0	2.8	93.7	0.17/0.065/0.03/0.01	35/30/35
SAC29	18.0	2.8	93.7	0.17/0.065/0.03/0.01	35/50/35
SAC30	18.0	2.8	93.7	0.17/0.065/0.03/0.01	35/70/35
SAC31	18.0	2.8	93.7	0.17/0.065/0.03/0.01	35/90/35
SAC32	18.0	2.8	71.4	0.17/0.065/0.03/0.01	35/30/35
SAC33	18.0	2.8	71.4	0.17/0.065/0.03/0.01	35/50/35
SAC34	18.0	2.8	71.4	0.17/0.065/0.03/0.01	35/70/35
SAC35	18.0	2.8	71.4	0.17/0.065/0.03/0.01	35/90/35

*All runs conducted with feed and column wall temperature of 308.15 K.

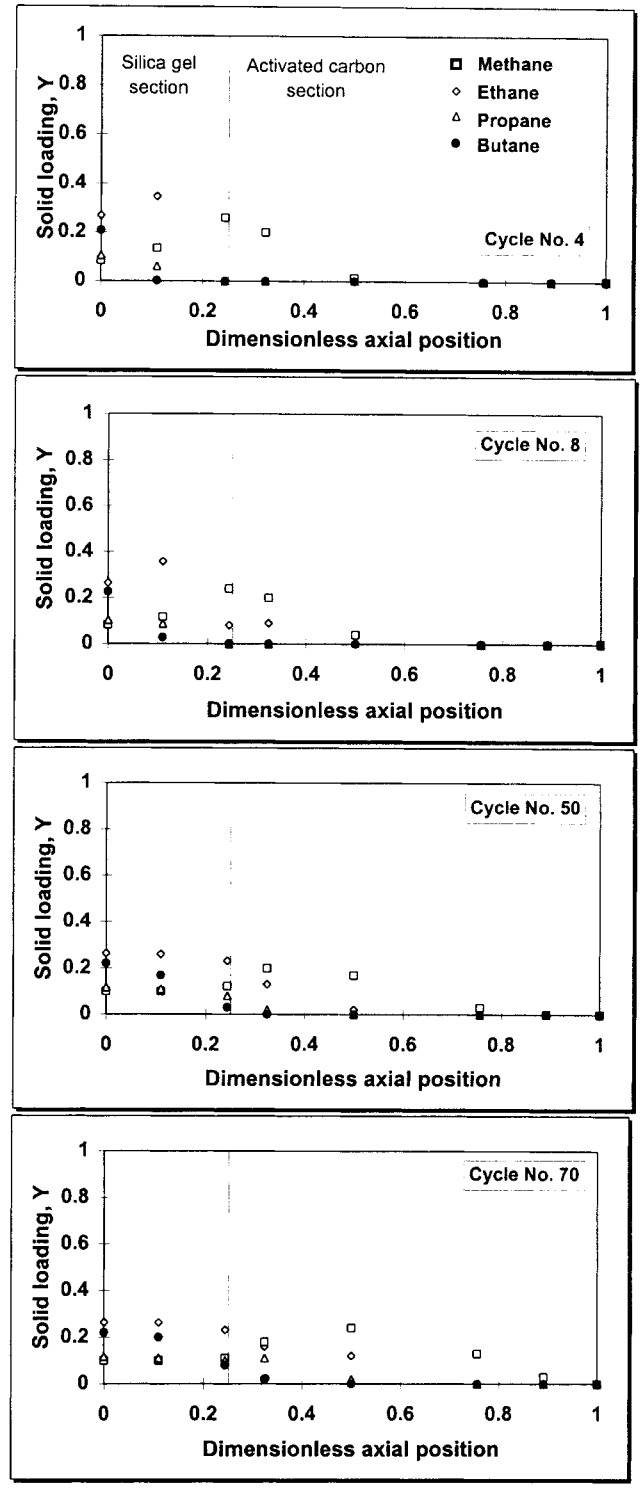

Figure 9. Penetration of hydrocarbon fronts in the PSA bed.

Run SAC25; operating conditions are given in Table 6; dotted line indicates the interface between silica gel and activated carbon sections.

Figure 9 for one of the simulation runs with a low feed velocity. In this case, the butane front is well retained within the silica gel section. Furthermore, there is no breakthrough of methane from the PSA bed. On the other hand, some pene-

tration of the butane front into the activated carbon section as well as partial breakthrough of the methane front at the bed exit were observed when the velocity was increased (for example, run SAC29 in Table 6).

It is interesting to note that the main effect of increasing feed velocity to the PSA unit for the same cycle time is the increasing distance penetrated by the various hydrocarbon concentration fronts in the bed during the high-pressure adsorption step. In particular, for the H_2-PSA system studied here, it is highly desirable to ensure that the butane front does not penetrate beyond the silica gel section and that the methane front is retained within the activated carbon section as the cycle progresses. As discussed earlier, butane adsorption on activated carbon is almost irreversible and significant penetration of the front beyond the silica gel section would, therefore, diminish the capacity of activated carbon for retaining the other (lighter) hydrocarbons as the PSA operation continues. Also, as shown earlier, the methane front in the bed is relatively sharp and a breakthrough of the front would result in a tremendous drop in product purity. Thus, a proper way of operating the H_2-PSA system for treatment of refinery fuel gas is to ensure the containment of the butane (and other heavier molecular weight hydrocarbons) within the silica gel section and the methane front (and, hence, the other hydrocarbon components) within the activated carbon section.

Conclusions

A comprehensive study of the performance of a multicomponent, six-bed, dual-sorbent PSA process for hydrogen purification from refinery fuel gases has been conducted. The PSA beds consist of an initial layer of silica gel used to trap heavier hydrocarbons and a second layer of activated carbon adsorbent to trap the lighter hydrocarbons. A simulation model of the process has been developed and verified based on some experiments performed using a laboratory-scale six-bed PSA unit.

Comparison between the single-sorbent (i.e., activated carbon only) and dual-sorbent operations indicates the advantage of the latter system where higher molecular weight hydrocarbons like butane are present in the feed. Butane is very strongly adsorbed on activated carbon and is difficult to desorb by simple pressure reduction. This is, however, not the case with its adsorption on silica gel. Hence, the initial layer of silica gel effectively prevents the gradual degradation of the activated carbon layer.

Other parametric studies show that the dual-sorbent system results in earlier breakthrough of the lighter hydrocarbons in contrast to single-sorbent operations due to a reduction in the total adsorptive capacity compared to the former system. In particular, it is pertinent to control the operating conditions so as to retain the butane front within the silica gel layer and the methane front within the activated carbon layer. Furthermore, comparison with isothermal simulation results reveals the importance of heat effects in the PSA beds for this process.

As a further study, the dual-sorbent model was modified to simulate an actual industrial six-bed H_2-PSA system in operation at a refinery in Singapore. Two important modifications were considered. The first is that the industrial operation is more realistically modeled as an adiabatic system since the heat-transfer area to volume ratio of the bed is relatively small. The second modification concerns the effect of hydrogen as the carrier gas in the industrial operation as compared to the use of helium in laboratory experiments. Helium had been used in the experiments as a matter of safety. Experimental studies show that the presence of hydrogen has little effect on the equilibrium and kinetics of hydrocarbon adsorption on activated carbon. However, hydrogen has a small adsorption capacity in activated carbon and its isotherm varies linearly with the partial pressure. Predictions of plant performance from the simulation model are in very good agreement with operating plant data. In addition, comparison with isothermal simulation results also reveal the importance of heat effects in the industrial operation. The simulation model will be useful for general PSA process studies as well as for the optimization of the plant performance.

Notation

b_o = equilibrium isotherm parameter, bar^{-1}
$D_{e,ave}$ = average effective diffusivity, cm^2/s
h_w = effective wall heat-transfer coefficient, $J/cm^2 \cdot s \cdot K$
K_0 = model parameter for linear equilibrium isotherm, mmol/g bar
L = column length, cm
q = adsorbed phase concentration, mmol/g
q^* = equilibrium adsorbed phase concentration, mmol/g
q_s^* = saturated equilibrium adsorbed phase concentration, mmol/g
q_{s1}^* = saturated equilibrium adsorbed phase concentration of methane in activated carbon, mmol/g
R = universal gas constant, = 8.314 J/mol·K
t_{c1}, t_{c2}, t_{c3} = duration of stages in a PSA cycle, s
T = temperature, K
v = interstitial gas velocity, cm/s
X = adsorbate mole fraction in gas phase
$Y = q/q_s^*$, dimensionless solid phase concentration
χ = dimensionless axial distance
$\gamma_i = q_{si}^*/q_{s1}^*$
$\theta = T/T_f$, dimensionless temperature
$\tau = v_f t/L$, dimensionless time
$(-\Delta H_A)$ = heat of adsorption, J/mol

Subscripts

B = adsorbent bed
1, 2, 3, 4 = methane, ethane, propane, and butane, respectively
f = feed or inlet conditions
i, k = adsorbate components in multicomponent adsorption

Literature Cited

Malek, A., "A Study of Hydrogen Purification from the Refinery Fuel Gas By Pressure Swing Adsorption," PhD Thesis, Dept. Chem. Eng., National University of Singapore (1996).

Malek, A., and S. Farooq, "Determination of Equilibrium Isotherms Using Dynamic Column Breakthrough and Constant Flow Equilibrium Desorption," *J. Chem. Eng. Data.*, **41**, 25 (1996a).

Malek, A., and S. Farooq, "Comparison of Isotherm Models for Hydrocarbon Adsorption on Activated Carbon," *AIChE J.*, **42**, 3191 (1996b).

Malek, A., and S. Farooq, "Kinetics of Hydrocarbon Adsorption on Activated Carbon and Silica Gel," *AIChE J.*, **43**, 761 (1997a).

Malek, A., and S. Farooq, "A Study of a 6-Bed Pressure Swing Adsorption Process," *AIChE J.*, **43**, 2509 (1997b).

Manuscript received Nov. 3, 1997, and revision received June 17, 1998.